

## Multiorder coherent Raman scattering of a quantum probe field

Fam Le Kien,\* Anil K. Patnaik, and K. Hakuta

*Department of Applied Physics and Chemistry, University of Electro-Communications, Chofu, Tokyo 182-8585, Japan*

(Received 26 March 2003; revised 29 July 2003; published 2 December 2003)

We study the multiorder coherent Raman scattering of a quantum probe field in a far-off-resonance medium with a prepared coherence. Under the conditions of negligible dispersion and limited bandwidth, we derive a Bessel-function solution for the sideband field operators. We analytically and numerically calculate various quantum statistical characteristics of the sideband fields. We show that the multiorder coherent Raman process can replicate the statistical properties of a single-mode quantum probe field into a broad comb of generated Raman sidebands. We also study the mixing and modulation of photon statistical properties in the case of two-mode input. We show that the prepared Raman coherence and the medium length can be used as control parameters to switch a sideband field from one type of photon statistics to another type, or from a nonsqueezed state to a squeezed state and vice versa. We demonstrate that an even or odd coherent state of the quantum probe field can produce a multipartite entangled coherent state. We show that the concurrence reaches its maximal value at an optimal medium length that is determined by the magnitude of the Raman coherence and the orders of the Raman sidebands.

DOI: 10.1103/PhysRevA.68.063803

PACS number(s): 42.50.Gy, 42.50.Dv, 42.65.Dr, 42.65.Ky

### I. INTRODUCTION

The parametric beating of a weak probe field with a prepared Raman coherence in a far-off-resonance medium has been extensively studied [1–4]. It has been demonstrated that multimode laser radiation [2] and incoherent fluorescent light [3] can be replicated into Raman sidebands. Since a substantial molecular coherence can be produced by the two-color adiabatic Raman pumping method [5–8], the quantum conversion efficiency of the parametric beating technique can be maintained high even for weak light with less than one photon per wave packet [3]. To describe the statistical properties of a weak quantum probe and its first-order Stokes and anti-Stokes sidebands in the parametric beating process, a simplified quantum treatment has recently been performed [9]. It has been shown that the statistical properties of the quantum probe can be replicated into the two sidebands nearest to the input line, in agreement with the experimental observations [2,3].

However, many experiments have reported the observations of ultrabroad Raman spectra with a large number of sidebands [2–6]. In the experiments with solid hydrogen [2,3], at least two anti-Stokes sidebands and two Stokes sidebands have been observed. In the experiment with molecular deuterium [6], a large Raman coherence  $|\rho_{ab}| \cong 0.33$  and about 20 Raman sidebands, covering a wide spectral range from near infrared through vacuum ultraviolet, have been generated. In rare-earth doped dielectrics with low Raman frequency and long-lived spin coherence, a substantial Raman coherence  $|\rho_{ab}| \cong 0.25$  and an extremely large number of sidebands (about  $10^4$ ) can also be generated [10]. Broad combs of Raman sidebands [2–6] have been intensively studied because they may synthesize to subfemtosecond

[7,8,11,12] and subcycle [13] pulses. The generation of broad combs of Raman sidebands has always been examined as a semiclassical problem. While classical treatments are sufficient for many purposes, a quantum treatment is required when the statistical properties of the radiation fields are important. On the other hand, broad combs of Raman sidebands with similar nonclassical properties and different frequencies may find useful applications for high-performance optical communication. Therefore it is intriguing to examine the quantum aspects of high-order coherent Raman processes.

In this paper, we study the multiorder coherent Raman scattering of a quantum probe field in a far-off-resonance medium with a prepared coherence. We calculate various quantum statistical characteristics of the sideband fields generated from a single-mode quantum input, study the mixing and modulation of photon statistical properties in the case of two-mode input, and investigate the generation of a multipartite entangled coherent state. Although the multiorder coherent Raman scattering has many similarities with a conventional beam splitter [14–19], the two systems are different in physical nature and, most importantly, the former can produce a broad comb of sideband fields with different frequencies. Therefore, in this paper, we also make comparison of our system with the conventional beam splitter as and when it is possible.

Before we proceed, we note that, in related problems, the generation of correlated photons using the  $\chi^{(2)}$  and  $\chi^{(3)}$  parametric processes has been studied [18–20]. The correlations between the Stokes and anti-Stokes sidebands and the possibility of transferring a quantum state of light from one carrier frequency to another carrier frequency (multiplexing) have been discussed for resonant systems [21].

The paper is organized as follows. In Sec. II, we describe the model and present the basic equations. In Sec. III, we study various quantum characteristics of the sideband fields generated from a single-mode quantum input. In Sec. IV, we discuss the quantum properties of the sideband fields gener-

---

\*On leave from Department of Physics, University of Hanoi, Hanoi, Vietnam. Also at Institute of Physics, National Center for Natural Sciences and Technology, Hanoi, Vietnam.

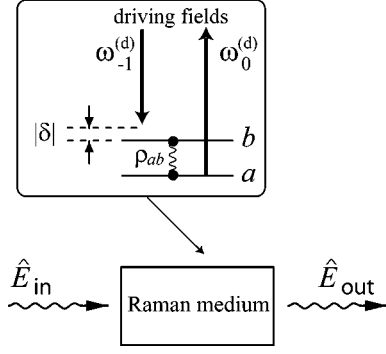


FIG. 1. Principle of the technique: Two classical laser fields drive a Raman transition of molecules in a far-off-resonance medium. The beating of a weak quantum probe field with the prepared Raman coherence produces new sideband fields.

ated from a two-mode quantum input. In Sec. V, we study the production of a multipartite entangled coherent state, and calculate the bipartite concurrence for the generated state. Finally, we present the conclusions in Sec. VI.

## II. MODEL

We consider a far-off-resonance Raman medium shown schematically in Fig. 1. Level  $a$  with energy  $\omega_a$  is coupled to level  $b$  with energy  $\omega_b$  by a Raman transition via intermediate levels that are not shown in the figure. We send a pair of long, strong, classical laser fields, with carrier frequencies  $\omega_{-1}^{(d)}$  and  $\omega_0^{(d)}$ , and a short, weak, quantum probe field  $\hat{E}_{in}$ , with one or several carrier frequencies, through the Raman medium, along the  $z$  direction. The timing and alignment of these fields are such that they substantially overlap with each other during the interaction process. The driving laser fields are tuned close to the Raman transition  $a \leftrightarrow b$ , with a small finite two-photon detuning  $\delta$ , but are far detuned from the upper electronic states  $j$  of the molecules. We assume that all the frequency components of the input probe field are separated by integer multiples of the Raman modulation frequency  $\omega_m = \omega_b - \omega_a - \delta$ . The driving fields adiabatically produce a Raman coherence  $\rho_{ab}$  [7,8]. When the probe field propagates through the medium, it beats with the prepared Raman coherence. Since the probe field is weak and short compared to the driving fields, the medium state and the driving fields do not change substantially during this step. The beating of the probe field with the prepared Raman coherence leads to the generation of new sidebands in the total output field  $\hat{E}_{out}$ . The frequencies of the sideband fields  $\hat{E}_q$  are given by  $\omega_q = \omega_0 + q\omega_m$ , where  $q$  is integer and  $\omega_0$  is a carrier frequency of the input probe field. The range of  $q$  should be appropriate so that  $\omega_q$  is positive. The probe field is taken to be not too short so that the Fourier-transformation limited broadening is negligible. We assume that the prepared Raman coherence  $\rho_{ab}$  is substantial so that the spontaneous Raman process is negligible compared to the stimulated and parametric processes. Consequently, the quantum noise can be neglected. Unlike Ref. [9], our model does not require any restriction on the magnitude of the coherence as

all Raman sidebands are included. When we take the propagation equation for the classical Raman sidebands [7,8] and replace the field amplitudes by the quantum operators, we obtain

$$\frac{\partial \hat{E}_q}{\partial z} + \frac{\partial \hat{E}_q}{c \partial t} = i\beta_q(u_q \hat{E}_q + d_{q-1} \rho_{ba} \hat{E}_{q-1} + d_q \rho_{ab} \hat{E}_{q+1}). \quad (1)$$

Here,  $u_q$  and  $d_q$  are the dispersion and coupling constants, respectively. We have denoted  $\beta_q = \mathcal{N} \hbar \omega_q / \epsilon_0 c$ , where  $\mathcal{N}$  is the molecular number density.

We take all the sidebands to be sufficiently far from resonance that the dispersion of the medium is negligible. In this case, we have  $u_q = u_0$  and  $d_q = d_0$ . We write

$$\rho_{ab} = \rho_0 \exp[i(\phi_0 - \beta_m u_0 z)], \quad (2)$$

where  $\rho_0 = |\rho_{ab}|$  and  $\beta_m = \mathcal{N} \hbar \omega_m / \epsilon_0 c$ , and assume that  $\rho_0$  and  $\phi_0$  are constant in time and space. We write the field amplitudes in terms of the photon operators as

$$\hat{E}_q = e^{i(\beta_q u_0 z - q \phi_0)} \sqrt{\frac{2 \hbar \omega_q}{\epsilon_0 L A}} \sum_K \hat{b}_q(K, t) e^{iK(z - ct)}. \quad (3)$$

Here,  $L$  is the quantization length taken to be equal to the medium length,  $A$  is the quantization transverse area taken to be equal to the beam area,  $K$  is a Bloch wave vector, and  $\hat{b}_q(K, t)$  and  $\hat{b}_q^\dagger(K, t)$  are the annihilation and creation operators for photons in the spectral mode  $q$  and the spatial mode  $K$ . Then, Eq. (1) yields

$$\frac{\partial \hat{b}_q}{\partial t} = i(g_q \hat{b}_{q-1} + g_{q+1} \hat{b}_{q+1}), \quad (4)$$

where  $g_q = (\mathcal{N} \hbar / \epsilon_0) \sqrt{\omega_q \omega_{q-1}} d_0 \rho_0$ . For the medium length  $L$ , the evolution time is  $t = L/c$ . For simplicity, we restrict our discussion to the case where each sideband field contains only a single spatial mode (with, e.g.,  $K=0$ ). It follows from Eq. (4) that the total photon number is conserved in time. Note that Eq. (4) represents the Heisenberg equation for the fields that are coupled to each other by the effective interaction Hamiltonian

$$\hat{H} = -\hbar \sum_q g_{q+1} (\hat{b}_q \hat{b}_{q+1}^\dagger + \hat{b}_{q+1} \hat{b}_q^\dagger). \quad (5)$$

The interaction between the sideband fields via the prepared Raman coherence is analogous to the interaction between the transmitted and reflected fields from a conventional beam splitter [19]. The two systems have the same underlying physics: the fields are linearly transformed from the input values. However, the two mechanisms are very different in physical nature. The most important difference between them is that the two fields from the conventional beam splitter have the same frequency while the sideband fields in the Raman scheme have different frequencies. In addition, the model Hamiltonian (5) involves an infinitely large number of Raman sidebands, separated by integer multiples of the Ra-

man modulation frequency  $\omega_m$ . Despite these differences, the model (5) can be called the multiorder Raman beam splitter.

Though we are dealing with quantum fields, the effective Hamiltonian (5) does not contain any Stark-shift terms, unlike the case of an atom with a two-photon transition inside an ideal cavity [22]. However, the dynamical Stark shift is not neglected in our model. The Stark shift caused by the strong classical driving fields affects the magnitudes of the Raman coherence  $\rho_{ab}$  and the level populations  $\rho_{aa}$  and  $\rho_{bb}$  [7,8]. When the dispersion is negligible, the phase of  $\rho_{ab}$  is modulated in space by the factor  $e^{-i\beta_m u_0 z}$  [see Eq. (2)], which leads to a shift for the phase velocity of the Raman polarization wave. The Stark shift caused by the quantum sideband fields  $\hat{E}_q$  is small compared to that caused by the strong classical driving fields. Therefore it does not affect the medium state. The propagation of  $\hat{E}_q$  can be described by an effective Hamiltonian that contains the Stark-shift term  $-\hbar \sum_q u_q \hat{E}_q^\dagger \hat{E}_q / 2$ . The signature of the Stark shift is the term  $i\beta_q u_q \hat{E}_q$  in Eq. (1). This term leads to a phase-velocity shift for the sideband  $q$ . Since  $u_q = u_0$  in the condition of negligible dispersion, this phase-velocity shift is the same for all the Raman sidebands. It is described by the phase factor  $e^{i\beta_q u_0 z}$  in the transformation (3), and is compensated by the phase-velocity shift of the Raman polarization wave. This explains why the effective Hamiltonian (5) for the propagation of the photon operators  $\hat{b}_q$  does not contain any Stark-shift terms. Such terms are also absent in the effective Hamiltonians for the propagating quantum fields generated in the parametric processes using classical nonresonant pump fields [19].

We assume that the bandwidth of the generated Raman spectrum is small compared to the characteristic probe frequency  $\omega_0$ . In this case, the  $q$  dependence of the coupling parameters  $g_q$  can be neglected, that is, we have  $g_q = g_0 = \mathcal{N} \hbar \omega_0 d_0 \rho_0 / \epsilon_0$ . With this assumption, we find the following solution to Eq. (4):

$$\hat{b}_q(t) = \sum_{q'} e^{i(q-q')\pi/2} J_{q-q'}(2g_0 t) \hat{b}_{q'}(0). \quad (6)$$

Here,  $J_k$  is the  $k$ th-order Bessel function. The expression (6) for the output field operators is a generalization of the Bessel-function solution obtained earlier for the classical fields [7,8]. The number of generated Raman sidebands is characterized by the effective interaction time  $2g_0 t$  or, equivalently, by the effective medium length  $\kappa L$ , where  $\kappa = 2g_0 / c = 2\hbar \mathcal{N} \omega_0 d_0 \rho_0 / \epsilon_0 c$ . The coefficient  $\kappa$  characterizes the strength of the parametric coupling and is proportional to the prepared Raman coherence  $\rho_0$ , that is, to the intensities of the driving laser fields. The Bessel functions  $J_k(\kappa L)$  are the transmission ( $k=0$ ) and scattering ( $k \neq 0$ ) coefficients for the Raman sidebands, similar to the transmission and reflection coefficients of a conventional beam splitter. The assumption of limited bandwidth requires  $\kappa L \ll \omega_0 / \omega_m$ , that is,  $(2\hbar / \epsilon_0 c) \mathcal{N} \omega_m d_0 \rho_0 L \ll 1$  [7,8].

### III. SINGLE-MODE QUANTUM INPUT

In this section, we consider the case where the input probe field has a single carrier frequency  $\omega_0$ . In other words, we assume that the sideband  $q=0$  is initially prepared in a quantum state  $\hat{\rho}_{\text{in}}^{(0)}$  and the other sidebands are initially in the vacuum state. The density matrix of the initial state of the fields is given by

$$\hat{\rho}_{\text{in}} = \hat{\rho}_{\text{in}}^{(0)} \otimes \prod_{q \neq 0} (|0\rangle\langle 0|)_q. \quad (7)$$

#### A. Autocorrelation functions

We study the autocorrelations of photons in the generated Raman sidebands. We use Eq. (6) and apply the initial density matrix (7) to calculate the normally ordered moments  $\langle \hat{b}_q^{\dagger n} \hat{b}_q^n \rangle$  of the photon-number operators  $\hat{n}_q = \hat{b}_q^\dagger \hat{b}_q$ . The result is

$$\langle \hat{b}_q^{\dagger n} \hat{b}_q^n \rangle = J_q^{2n}(\kappa L) \langle \hat{b}_0^{\dagger n}(0) \hat{b}_0^n(0) \rangle. \quad (8)$$

In particular, the mean photon numbers of the sidebands are given by

$$\langle \hat{n}_q \rangle = J_q^2(\kappa L) \langle \hat{n}_{\text{in}} \rangle. \quad (9)$$

Here,  $\hat{n}_{\text{in}} = \hat{b}_0^\dagger(0) \hat{b}_0(0)$  is the photon-number operator for the input field. The  $n$ th-order autocorrelation functions of the sidebands are defined by  $\Gamma_q^{(n)} = \langle \hat{b}_q^{\dagger n} \hat{b}_q^n \rangle - \langle \hat{b}_q^\dagger \hat{b}_q \rangle^n$ . From Eqs. (8) and (9), we find

$$\Gamma_q^{(n)} = J_q^{2n}(\kappa L) \Gamma_{\text{in}}^{(n)}, \quad (10)$$

where  $\Gamma_{\text{in}}^{(n)} = \langle \hat{b}_0^{\dagger n}(0) \hat{b}_0^n(0) \rangle - \langle \hat{b}_0^\dagger(0) \hat{b}_0(0) \rangle^n$  is the  $n$ th-order autocorrelation function of the input field.

Equations (9) and (10) indicate that, when we increase the effective medium length  $\kappa L$  or the sideband order  $q$ , the mean photon number  $\langle \hat{n}_q \rangle$  and the autocorrelation function  $\Gamma_q^{(n)}$  undergo oscillations as described by even powers of the Bessel function  $J_q(\kappa L)$ . Such oscillatory behavior is illustrated in Fig. 2. When the sideband order  $q$  is higher, the onset of  $\langle \hat{n}_q \rangle$  occurs later [see Fig. 2(a)] and hence so does the onset of  $\Gamma_q^{(n)}$  [see Fig. 2(c)]. For a fixed order  $q$ , both  $\langle \hat{n}_q \rangle$  and  $\Gamma_q^{(n)}$  reach their largest values at the same optimal medium length  $L_q = x_q / \kappa$ , where  $x_q$  is the position of the first peak of  $J_q(x)$ . The higher the sideband order  $q$ , the larger is the optimal length  $L_q$  and the smaller are the maximal output values of  $\langle \hat{n}_q \rangle$  and  $\Gamma_q^{(n)}$  [see Figs. 2(a) and (c)]. Figures 2(b) and (d) show that  $\langle \hat{n}_q \rangle$  and  $\Gamma_q^{(n)}$  are substantially different from zero only in the region where  $|q|$  is not too large compared to  $\kappa L$ . For a given  $\kappa L$ , both  $\langle \hat{n}_q \rangle$  and  $\Gamma_q^{(n)}$  achieve their maximal values at  $q \approx \kappa L$ .

The normalized  $n$ th-order autocorrelation functions of the sidebands are defined by  $g_q^{(n)} = \langle \hat{b}_q^{\dagger n} \hat{b}_q^n \rangle / \langle \hat{b}_q^\dagger \hat{b}_q \rangle^n$ . These functions characterize the overall statistical properties, such as sub-Poissonian, Poissonian, or super-Poissonian photon

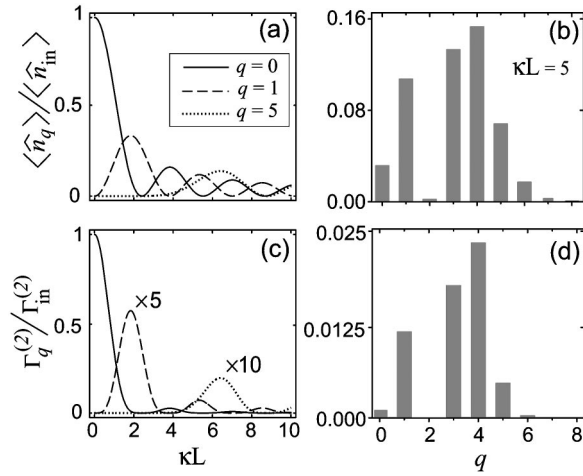


FIG. 2. Mean photon number  $\langle \hat{n}_q \rangle$  (first row) and second-order autocorrelation function  $\Gamma_q^{(2)}$  (second row), both scaled to their initial values for the probe field, as functions of the effective medium length  $\kappa L$  (first column) and the sideband order  $q$  (second column). In (a) and (c), the sideband order is 0 (solid line), 1 (dashed line), and 5 (dotted line). In (b) and (d), the effective medium length is  $\kappa L=5$ . In (c), we have amplified  $\Gamma_1^{(2)}/\Gamma_{in}^{(2)}$  (dashed line) and  $\Gamma_5^{(2)}/\Gamma_{in}^{(2)}$  (dotted line) by five and ten times, respectively. In (b) and (d), the negative side of the  $q$  axis is not shown because the functions plotted are symmetric in  $q$ .

statistics, regardless of the mean photon number. Unlike the mean photon number  $\langle \hat{n}_q \rangle$  and the autocorrelation function  $\Gamma_q^{(n)}$ , the normalized autocorrelation function  $g_q^{(n)}$  does not oscillate when we change the effective medium length  $\kappa L$  or the sideband order  $q$ . Indeed, with the help of Eq. (8), we find [9]  $g_q^{(n)} = g_{in}^{(n)}$ , where  $g_{in}^{(n)} = \langle \hat{b}_0^{\dagger n}(0) \hat{b}_0^n(0) \rangle / \langle \hat{b}_0^{\dagger}(0) \hat{b}_0(0) \rangle^n$ . Thus the generated sideband fields and the probe field have the same normalized autocorrelation functions, which are independent of the evolution time and are solely determined by the statistical properties of the input field. In other words, the normalized autocorrelation functions of the probe field do not change during the parametric beating process and are precisely replicated into the comb of generated sidebands. Such a replication of the normalized autocorrelation characteristics can be called autocorrelation multiplexing. This result is in agreement with the experiments on replication of multimode laser radiation [2] and broadband incoherent light [3]. The ability of the Raman medium to replicate the autocorrelation characteristics is similar to that of a conventional beam splitter [19].

It is not surprising that the normalized autocorrelation functions of the probe field are replicated into the sidebands in the parametric beating process. Such a replication is possible because the medium is far off resonance and the quantum probe field is weak compared to the driving fields. Under these two conditions, the photon annihilation operators are linearly transformed as described by the linear differential equation (4). This equation shows that the photon annihilation operators are not mixed up with the creation operators, and therefore the evolution of the annihilation operators is linear with respect to the initial annihilation operators.

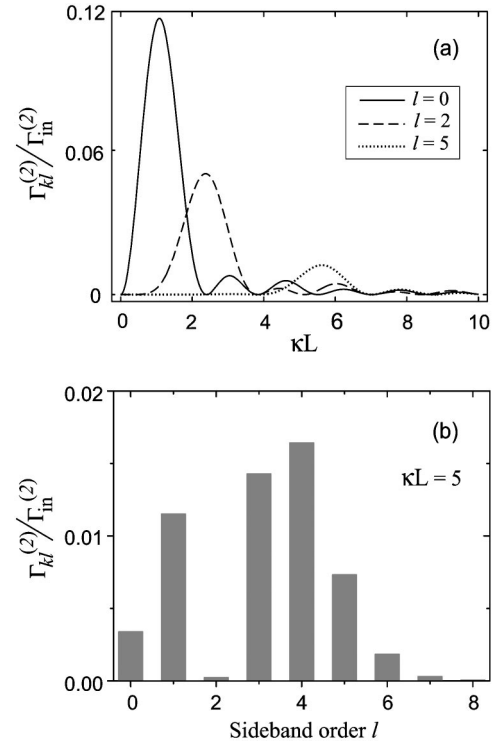


FIG. 3. Cross-correlation function  $\Gamma_{kl}^{(2)}$ , scaled with the second-order autocorrelation function of the input field, as a function of (a) the effective medium length  $\kappa L$  and (b) the sideband order  $l$ . Here, the sideband order  $k$  is fixed to 1. In (a), the sideband order  $l$  is 0 (solid line), 2 (dashed line), and 5 (dotted line). In (b), the effective medium length is  $\kappa L=5$ . In (b), the negative side of the  $l$  axis is not shown because the function plotted is symmetric with respect to the sideband orders.

## B. Cross-correlation functions

We study the correlations between the generated Raman sidebands. For two different sidebands  $k$  and  $l$  ( $k \neq l$ ), we have

$$\langle \hat{n}_k \hat{n}_l \rangle = J_k^2(\kappa L) J_l^2(\kappa L) \langle \hat{n}_{in}(\hat{n}_{in} - 1) \rangle. \quad (11)$$

The cross-correlation function for the two sidebands is defined by  $\Gamma_{kl}^{(2)} = \langle \hat{n}_k \hat{n}_l \rangle - \langle \hat{n}_k \rangle \langle \hat{n}_l \rangle$ . Using Eqs. (9) and (11), we find

$$\Gamma_{kl}^{(2)} = J_k^2(\kappa L) J_l^2(\kappa L) \Gamma_{in}^{(2)}. \quad (12)$$

When we extend  $\Gamma_{kl}^{(2)}$  for  $k=l$ , we have  $\Gamma_{kk}^{(2)} = \Gamma_k^{(2)}$ . According to Eq. (12), the cross-correlation function  $\Gamma_{kl}^{(2)}$  oscillates when we change the effective medium length  $\kappa L$  or the sideband orders  $k$  and  $l$ . Such oscillatory behavior is illustrated in Fig. 3.

The normalized cross-correlation function is defined by  $g_{kl}^{(2)} = \langle \hat{n}_k \hat{n}_l \rangle / (\langle \hat{n}_k \rangle \langle \hat{n}_l \rangle)$ . Unlike the function  $\Gamma_{kl}^{(2)}$ , the normalized function  $g_{kl}^{(2)}$  does not oscillate. Indeed, we find the relation [9]  $g_{kl}^{(2)} = g_q^{(2)} = g_{in}^{(2)}$ . Thus the normalized cross-correlation functions  $g_{kl}^{(2)}$  for all possible sideband pairs  $(k, l)$  are equal to each other, to the normalized second-order au-

to correlation function  $g_q^{(2)}$  for each sideband  $q$ , and to the normalized second-order autocorrelation function  $g_{\text{in}}^{(2)}$  of the input field. When  $g_{\text{in}}^{(2)} \neq 1$ , that is, when the photon statistics of the input field is non-Poissonian, we obtain  $g_{kl}^{(2)} \neq 1$ , a signature of cross correlations between the sidebands. Such correlations are generated although the sidebands are initially not correlated. In particular, if the input field has a sub-Poissonian photon statistics ( $g_{\text{in}}^{(2)} < 1$ ), anticorrelations between the sidebands ( $g_{kl}^{(2)} < 1$ ) will be generated. Note that the conventional beam splitters also have a similar property [19].

### C. Squeezing

We examine the squeezing of the field quadratures. A field quadrature of the  $q$ th mode is defined by  $\hat{X}_q = \hat{b}_q^\dagger e^{i\varphi} + \hat{b}_q e^{-i\varphi}$ . We say that the  $q$ th mode is in a squeezed state if there exists such a phase  $\varphi$  that  $\langle (\Delta \hat{X}_q)^2 \rangle < 1$  or, equivalently,  $S_q < 0$ , where  $S_q = \langle (\Delta \hat{X}_q)^2 \rangle - 1$ . The squeezing degree is measured by the quantity  $-S_q$ . Note that the relation between the squeezing factor  $S_q$  and the conventional squeezing parameter  $r_q$  is  $S_q = e^{-2r_q} - 1$ . In terms of the photon operators, we have

$$S_q = 2[\langle \hat{b}_q^\dagger \hat{b}_q \rangle - \langle \hat{b}_q^\dagger \rangle \langle \hat{b}_q \rangle] + [\langle \hat{b}_q^2 \rangle - \langle \hat{b}_q \rangle^2] e^{-2i\varphi} + \text{c.c.} \quad (13)$$

With the help of Eqs. (6) and (7), we find

$$S_q(\varphi + q\pi/2) = J_q^2(\kappa L) S_{\text{in}}(\varphi). \quad (14)$$

Here,  $S_{\text{in}}(\varphi)$  denotes the squeezing factor for the  $\varphi$  quadrature of the input field. Equation (14) shows that, if  $S_{\text{in}}(\varphi) < 0$ , then  $S_q(\varphi + q\pi/2) < 0$ . Thus the squeezing of the input field can be transferred to the comb of generated sidebands by the parametric beating process. The squeezing factor  $S_q(\varphi + q\pi/2)$  of the sideband  $q$  is reduced from the input squeezing factor  $S_{\text{in}}(\varphi)$  by the factor  $J_q^2(\kappa L)$ . Unlike the case of linear directional couplers and beam splitters [18], the squeezing degree of the probe field cannot be completely transferred to the Raman sidebands. This difference is due to the fact that the linear directional coupler and the beam splitter involve only two output modes while the multiorder coherent Raman process involves many more output modes. Note that the phase of the squeezed quadrature of the sideband  $q$  changes by  $q\pi/2$ . This means that the squeezed quadrature of a generated even-order (odd-order) Raman sideband is parallel (orthogonal) to that of the input field.

We introduce the normalized squeezing factor  $s_q = S_q / \langle \hat{n}_q \rangle$ . We find the relation [9]  $s_q(\varphi + q\pi/2) = s_{\text{in}}(\varphi)$ , where  $s_{\text{in}}(\varphi) = S_{\text{in}}(\varphi) / \langle \hat{n}_{\text{in}} \rangle$  is the normalized squeezing factor for the input field. Thus besides a shift of the quadrature phase angle, the normalized squeezing factor for the input field is replicated into the comb of generated sidebands. This result can be used to convert squeezing to a new frequency, i.e., to perform squeezing multiplexing. The relation  $S_q(\varphi + q\pi/2) / S_{\text{in}}(\varphi) = \langle \hat{n}_q \rangle / \langle \hat{n}_{\text{in}} \rangle$  indicates that the  $\kappa L$  and  $q$  dependences of the squeezing factor  $S_q(\varphi + q\pi/2)$  are similar

to those of the mean photon number  $\langle \hat{n}_q \rangle$  [see Figs. 2(a) and (b)]. Note that, when the input field is in a coherent state, the sideband fields have no squeezing. This property is similar to the case of four-wave mixing but is unlike the case of degenerate parametric down-conversion, where perfect squeezing can in principle be obtained.

### D. Photon distributions and quantum states of the output fields

We calculate the photon distributions and quantum states of the output fields. We first consider the case where the input sideband 0 is initially prepared in a Fock state  $|N\rangle_0$ . The input state of the total field is written as

$$|\Psi_{\text{in}}\rangle = |N\rangle_0 \prod_{q \neq 0} |0\rangle_q = \frac{1}{\sqrt{N!}} \hat{b}_0^{\dagger N} |0\rangle |0\rangle. \quad (15)$$

The output state of the total field is given by  $|\Psi_{\text{out}}\rangle = (N!)^{-1/2} \hat{b}_0^{\dagger N} (-L/c) |0\rangle$ . With the help of Eq. (6), we find

$$|\Psi_{\text{out}}\rangle = \sum_{\{n_q\}} C_{\{n_q\}}^{(N)} |\{n_q\}\rangle. \quad (16)$$

Here,

$$C_{\{n_q\}}^{(N)} = \sqrt{\frac{N!}{\prod_q n_q!}} \prod_q e^{iqn_q\pi/2} J_q^{n_q}(\kappa L) \quad (17)$$

for  $\sum_q n_q = N$ , and  $C_{\{n_q\}}^{(N)} = 0$  for  $\sum_q n_q \neq N$ . When  $N \neq 0$  and  $\kappa L \neq 0$ , the output state (16) is, in general, a multipartite inseparable (entangled) state. In a particular case where the input state of the probe field is a single-photon state, i.e.,  $N = 1$ , Eqs. (16) and (17) yield  $|\Psi_{\text{out}}\rangle = |W_R\rangle \equiv \sum_q e^{iq\pi/2} J_q(\kappa L) |1_q\rangle$ . Here,  $|1_q\rangle$  is the quantum state of a single photon in the sideband  $q$  with no photons in the other sidebands.

With the help of the above result, we can easily calculate the output state  $\hat{\rho}_{\text{out}}$  generated from an arbitrary state  $\hat{\rho}_{\text{in}}^{(0)}$  of the input mode 0. For the joint photon distribution of the output fields  $P_{\Sigma}(\{n_q\}) = \langle \{n_q\} | \hat{\rho}_{\text{out}} | \{n_q\} \rangle$ , we find

$$P_{\Sigma}(\{n_q\}) = p_{\text{in}}(N) \frac{N!}{\prod_q n_q!} \prod_q J_q^{2n_q}(\kappa L), \quad (18)$$

where  $p_{\text{in}}(n) = {}_0\langle n | \hat{\rho}_{\text{in}}^{(0)} | n \rangle_0$  is the photon distribution of the input mode, and  $N = \sum_q n_q$  is the total number of photons in the modes. From Eq. (18), the marginal photon distribution  $p_q(n)$  for the sideband  $q$  is obtained as

$$p_q(n) = \frac{J_q^{2n}(\kappa L)}{n!} \sum_{k=0}^{\infty} \frac{(n+k)!}{k!} [1 - J_q^2(\kappa L)]^k p_{\text{in}}(n+k). \quad (19)$$

Clearly,  $p_q(n)$  is in general different from  $p_{\text{in}}(n)$ . When the probe field is initially in a Fock state  $|N\rangle_0$ , we find

$$p_q(n) = J_q^{2n}(\kappa L) [1 - J_q^2(\kappa L)]^{N-n} \frac{N!}{n!(N-n)!} \quad (20)$$

for  $n \leq N$ , and  $p_q(n) = 0$  for  $n > N$ .

When the input sideband 0 is initially in a coherent state  $|\alpha\rangle_0$ , the state of the fields at the output is given by  $|\Psi_{\text{out}}\rangle = |\{\alpha_q(L/c)\}\rangle \equiv \prod_q |\alpha_q(L/c)\rangle_q$ . Here,  $|\alpha_q(L/c)\rangle_q$  is a coherent state of the  $q$ th mode, with the amplitude  $\alpha_q(L/c) = \alpha J_q(\kappa L) e^{iq\pi/2}$ . Thus a probe field in a coherent state can produce sideband fields that are also in coherent states but have different frequencies. Such a process can be called coherent-state multiplexing. The ability of the Raman medium to replicate a coherent state is similar to that of a conventional beam splitter [19].

When the input sideband 0 is initially in an incoherent mixed state

$$\hat{\rho}_{\text{in}}^{(0)} = \sum_n p_{\text{in}}(n) (|n\rangle\langle n|)_0, \quad (21)$$

the density matrix of the output state of the fields is found to be

$$\hat{\rho}_{\text{out}} = \sum_{N, \{n_q\}, \{n'_q\}} p_{\text{in}}(N) C_{\{n_q\}}^{(N)} C_{\{n'_q\}}^{(N)*} |\{n_q\}\rangle\langle\{n'_q\}|. \quad (22)$$

The reduced density matrix  $\hat{\rho}_{\text{out}}^{(q)}$  for an arbitrary sideband  $q$  is  $\hat{\rho}_{\text{out}}^{(q)} = \sum_n p_q(n) (|n\rangle\langle n|)_q$ . As seen, the reduced state of each sideband is also an incoherent superposition of Fock states. Note that, in general, we have  $\hat{\rho}_{\text{out}} \neq \prod_q \hat{\rho}_{\text{out}}^{(q)}$ .

#### IV. TWO-MODE QUANTUM INPUT

A far-off-resonance medium with a substantial Raman coherence, prepared by two strong driving fields, can efficiently mix and modulate the quantum statistical properties of the sideband fields. To understand this mechanism, we study the case where the input probe field has two carrier frequencies,  $\omega_0$  and  $\omega_\nu = \omega_0 + \nu\omega_m$ , separated by an integer multiple  $\nu$  of the Raman modulation frequency  $\omega_m$ . We assume that the Raman sidebands 0 and  $\nu$  are initially in independent quantum states  $\hat{\rho}_{\text{in}}^{(0)}$  and  $\hat{\rho}_{\text{in}}^{(\nu)}$ , respectively, while the other sidebands are initially in the vacuum state. The density matrix of the initial state of the fields is given by

$$\hat{\rho}_{\text{in}} = \hat{\rho}_{\text{in}}^{(0)} \otimes \hat{\rho}_{\text{in}}^{(\nu)} \otimes \prod_{q \neq 0, \nu} (|0\rangle\langle 0|)_q. \quad (23)$$

Here,  $\nu \neq 0$ .

##### A. Modulation of photon statistics

We study the mixing and modulation of photon statistics of the sideband fields. When we use Eq. (6) to calculate the mean photon numbers of the sidebands generated from the initial state (23), we find

$$\begin{aligned} \langle \hat{n}_q \rangle &= J_q^2(\kappa L) \langle \hat{b}_0^\dagger(0) \hat{b}_0(0) \rangle + J_{q-\nu}^2(\kappa L) \langle \hat{b}_\nu^\dagger(0) \hat{b}_\nu(0) \rangle \\ &+ J_q(\kappa L) J_{q-\nu}(\kappa L) [e^{-i\nu\pi/2} \langle \hat{b}_0^\dagger(0) \rangle \langle \hat{b}_\nu(0) \rangle + \text{c.c.}], \end{aligned} \quad (24)$$

Furthermore, the second-order autocorrelation function  $\Gamma_q^{(2)} = \langle \hat{b}_q^{\dagger 2} \hat{b}_q^2 \rangle - \langle \hat{b}_q^\dagger \hat{b}_q \rangle^2$  of the sideband  $q$  is found to be

$$\begin{aligned} \Gamma_q^{(2)} &= J_q^4(\kappa L) \Gamma_0^{(2)}(0) + J_{q-\nu}^4(\kappa L) \Gamma_\nu^{(2)}(0) \\ &+ 2J_q^2(\kappa L) J_{q-\nu}^2(\kappa L) \Delta_0 + [e^{-i\nu\pi} J_q^2(\kappa L) J_{q-\nu}^2(\kappa L) \Delta_1 \\ &+ 2e^{-i\nu\pi/2} J_q^3(\kappa L) J_{q-\nu}(\kappa L) \Delta_2 \\ &+ 2e^{-i\nu\pi/2} J_q(\kappa L) J_{q-\nu}^3(\kappa L) \Delta_3 + \text{c.c.}], \end{aligned} \quad (25)$$

where

$$\begin{aligned} \Delta_0 &= \langle \hat{b}_0^\dagger(0) \hat{b}_0(0) \rangle \langle \hat{b}_\nu^\dagger(0) \hat{b}_\nu(0) \rangle - |\langle \hat{b}_0(0) \rangle|^2 |\langle \hat{b}_\nu(0) \rangle|^2, \\ \Delta_1 &= \langle \hat{b}_0^{\dagger 2}(0) \rangle \langle \hat{b}_\nu^2(0) \rangle - \langle \hat{b}_0^\dagger(0) \rangle^2 \langle \hat{b}_\nu(0) \rangle^2, \\ \Delta_2 &= \langle \hat{b}_\nu(0) \rangle [\langle \hat{b}_0^{\dagger 2}(0) \hat{b}_0(0) \rangle - \langle \hat{b}_0^\dagger(0) \hat{b}_0(0) \rangle \langle \hat{b}_0^\dagger(0) \rangle], \\ \Delta_3 &= \langle \hat{b}_0^\dagger(0) \rangle [\langle \hat{b}_\nu^\dagger(0) \hat{b}_\nu^2(0) \rangle - \langle \hat{b}_\nu^\dagger(0) \hat{b}_\nu(0) \rangle \langle \hat{b}_\nu(0) \rangle]. \end{aligned} \quad (26)$$

The first two terms on the right-hand sides of Eqs. (24) and (25) are the individual contributions of the input sidebands 0 and  $\nu$ . The other terms result from the interference between the two interaction channels.

Unlike the case of single-mode input, in the case of two-mode input, the normalized second-order autocorrelation function  $g_q^{(2)} = 1 + \Gamma_q^{(2)} / \langle \hat{n}_q \rangle^2$  depends, in general, on  $\kappa L$  and  $q$ . Such behavior is illustrated in Fig. 4. When  $\kappa L$  is such that  $J_q(\kappa L) = 0$  or  $J_{q-\nu}(\kappa L) = 0$ , we have  $g_q^{(2)} = g_\nu^{(2)}(0)$  or  $g_q^{(2)} = g_0^{(2)}(0)$ , respectively. Consequently, if the two input sidebands have different normalized autocorrelation functions, i.e.,  $g_0^{(2)}(0) \neq g_\nu^{(2)}(0)$ , then, with increasing  $\kappa L$  or  $q$ , the normalized autocorrelation function  $g_q^{(2)}$  will oscillate between the values  $g_0^{(2)}(0)$  and  $g_\nu^{(2)}(0)$  (see Fig. 4). In particular, if the photon statistics of one of the input fields, e.g., the sideband 0, is sub-Poissonian [ $g_0^{(2)}(0) < 1$ ] and that of the other input field is super-Poissonian [ $g_\nu^{(2)}(0) > 1$ ], then each generated sideband  $q$  will have complex statistical properties and will oscillate between sub-Poissonian [ $g_q^{(2)} < 1$ ] and super-Poissonian [ $g_q^{(2)} > 1$ ] photon statistics (see Fig. 4). Using the prepared Raman coherence  $\rho_0$  or the medium length  $L$  as a control parameter, we can switch a sideband field from super-Poissonian photon statistics to sub-Poissonian or vice versa. Similar modulation of photon statistics has been demonstrated in a linear directional coupler [18].

##### B. Modulation of squeezing

We study the mixing and modulation of the squeezing properties of the sideband fields. When we use Eq. (6) to calculate the squeezing factor (13) for the sidebands generated from the initial state (23), we find

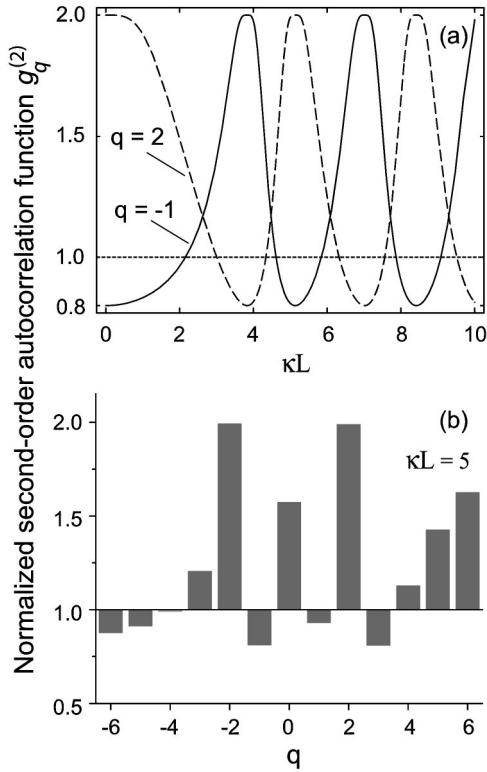


FIG. 4. Normalized second-order autocorrelation function  $g_q^{(2)}$  as a function of (a) the effective medium length  $\kappa L$  and (b) the sideband order  $q$  in the case of two-mode input. The input sideband 0 is initially prepared in a Fock state, with five photons. The input sideband 1 is initially prepared in a thermal state, with 1 photon in average. In (a), the sideband order is  $-1$  (solid line) and  $2$  (dashed line). In (b), the effective medium length is  $\kappa L = 5$ .

$$S_q(\varphi + q\pi/2) = J_q^2(\kappa L)S_0^{(\text{in})}(\varphi) + J_{q-\nu}^2(\kappa L)S_\nu^{(\text{in})}(\varphi + \nu\pi/2), \quad (27)$$

where  $S_0^{(\text{in})}$  and  $S_\nu^{(\text{in})}$  are the initial squeezing factors of the sidebands 0 and  $\nu$ , respectively. As seen, the squeezing factor  $S_q$  of the sideband  $q$  is a superposition of the input squeezing factors  $S_0^{(\text{in})}$  and  $S_\nu^{(\text{in})}$ , taken with the quadrature phase shifts  $-q\pi/2$  and  $-(q-\nu)\pi/2$ , respectively, and weighted by the factors  $J_q^2(\kappa L)$  and  $J_{q-\nu}^2(\kappa L)$ , respectively.

Unlike the case of single-mode input, in the case of two-mode input, the normalized squeezing factor  $s_q(\varphi + q\pi/2) = S_q(\varphi + q\pi/2)/\langle \hat{n}_q \rangle$  varies, in general, with  $\kappa L$  and  $q$ . Such behavior is illustrated in Fig. 5. When  $\kappa L$  is such that  $J_q(\kappa L) = 0$  or  $J_{q-\nu}(\kappa L) = 0$ , we have  $s_q(\varphi + q\pi/2) = s_\nu^{(\text{in})}(\varphi + \nu\pi/2)$  or  $s_q(\varphi + q\pi/2) = s_0^{(\text{in})}(\varphi)$ , respectively. Consequently, if the normalized squeezing factors  $s_0^{(\text{in})}(\varphi)$  and  $s_\nu^{(\text{in})}(\varphi + \nu\pi/2)$  of the two input fields are different, the normalized squeezing factor  $s_q(\varphi + q\pi/2)$  will oscillate between the values  $s_0^{(\text{in})}(\varphi)$  and  $s_\nu^{(\text{in})}(\varphi + \nu\pi/2)$ . In particular, if one of the two input fields, e.g., the sideband 0, is squeezed [ $s_0^{(\text{in})}(\varphi) < 0$ ] and the other input field is not squeezed [ $s_\nu^{(\text{in})}(\varphi) > 0$ ], then, each generated sideband  $q$  will have complex squeezing properties and will oscillate between a squeezed state [ $s_q(\varphi + q\pi/2) < 0$ ] and a non-

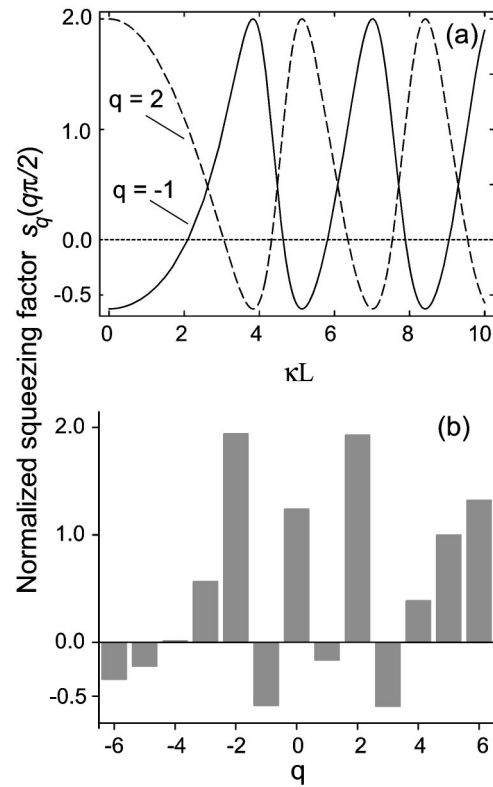


FIG. 5. Normalized squeezing factor  $s_q(q\pi/2)$  as a function of (a) the effective medium length  $\kappa L$  and (b) the sideband order  $q$  in the case of two-mode input. The input sideband 0 is initially prepared in a squeezed vacuum state, with the squeezing parameter  $r = 1$  and the phase  $\theta = 0$ . The input sideband 1 is initially prepared in a thermal state, with the mean photon number 1. In (a), the sideband order is  $-1$  (solid line) and  $2$  (dashed line). In (b), the effective medium length is  $\kappa L = 5$ .

squeezed state [ $s_q(\varphi) > 0$ ], see Fig. 5. Using the prepared Raman coherence  $\rho_0$  or the medium length  $L$  as a control parameter, we can switch a sideband field from a non-squeezed state to a squeezed state or vice versa. Note that a similar result has been obtained for a linear directional coupler [18].

We analyze a particular case where the sideband 0 is initially in a squeezed vacuum state  $|\xi\rangle_0 = \exp[(\xi^* \hat{b}_0^2 - \xi \hat{b}_0^{+2})/2]|0\rangle_0$  and the sideband  $\nu$  is initially in a coherent state  $|\alpha\rangle_\nu$ . Here,  $\xi = r e^{i\theta}$  is a complex number, the modulus  $r = |\xi|$  characterizes the amount of squeezing, and the phase angle  $\theta$  characterizes the alignment of the squeezed vacuum state in phase space. Then, we find from Eq. (24) the mean photon number

$$\langle \hat{n}_q \rangle = J_q^2(\kappa L) \sinh^2 r + J_{q-\nu}^2(\kappa L) |\alpha|^2. \quad (28)$$

We find from Eq. (27) that the maximal squeezing of the sideband  $q$  occurs in the  $\varphi_q$  quadrature where  $\varphi_q = \theta/2 + q\pi/2$ . The corresponding value of the squeezing factor is

$$S_q(\varphi_q) = J_q^2(\kappa L) (e^{-2r} - 1). \quad (29)$$

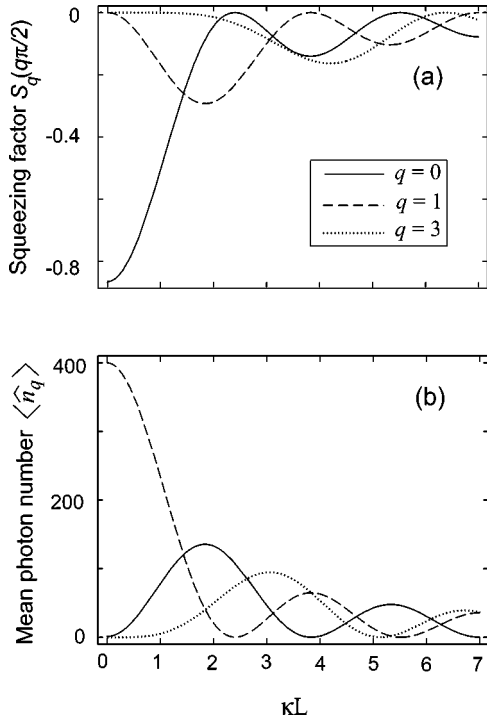


FIG. 6. (a) Squeezing factor  $S_q(q\pi/2)$  and (b) mean photon number  $\langle \hat{n}_q \rangle$  as functions of the effective medium length  $\kappa L$  in the case where the sideband 0 is initially prepared in a weak squeezed vacuum state and the sideband 1 is initially prepared in a strong coherent state. The parameters for the initial states of the input sidebands are  $r=1$ ,  $\theta=0$ , and  $\alpha=20$ . The curves are calculated for the sidebands 0 (solid line), 1 (dashed line), and 3 (dotted line).

As seen from Eq. (29), squeezing can be transferred from the initial squeezed vacuum state of the sideband 0 to the other sidebands. The squeezing factors of the sidebands are independent of the amplitude  $\alpha$  of the initial coherent state of the sideband  $\nu$ . Meanwhile, the mean photon number of each sideband is governed not only by the squeezing parameter  $r$  of the initial state of the sideband 0 but also by the amplitude  $\alpha$  of the initial state of the sideband  $\nu$ . Using this fact, we can manipulate to get optimized mean photon numbers and squeezing degrees of the sideband fields at the output as per requirement. In particular, we can convert squeezing from a weak field to a much stronger field. To illustrate this possibility, we plot in Fig. 6 the squeezing factor  $S_q(q\pi/2)$  and the mean photon number  $\langle \hat{n}_q \rangle$  as functions of the effective medium length  $\kappa L$  for the parameters  $r=1$ ,  $\theta=0$ ,  $\nu=1$ , and  $\alpha=20$ . In this case, the most negative value of the input squeezing factor  $S_0^{(in)}(\varphi)$  is achieved at  $\varphi=0$  and is given by  $S_0^{(in)}(0) = e^{-2r} - 1 \cong -0.86$ , indicating the squeezing degree 86%. The mean photon number of the input squeezed vacuum state is  $\langle \hat{n}_0(0) \rangle = \sinh^2 r \cong 1.38$ , rather small. The solid lines in Fig. 6 show that the sideband 0, initially prepared in a weak squeezed vacuum state, can be significantly enhanced while keeping its squeezing degree substantial. Meanwhile, the dashed lines show that, for  $\kappa L = 1.84$ , the sideband 1, initially prepared in a strong coherent state, is squeezed by about 29% and has the mean photon number of about 41. Similarly, the dotted lines show that, for  $\kappa L$

$= 4.2$ , a generated new sideband 3 is squeezed by about 16% and has the mean photon number of about 39. Thus, from a weak squeezed field at the input, we can obtain other output squeezed fields that have smaller but still substantial squeezing degrees, much larger mean photon numbers, and different frequencies.

### C. Two-photon interference

We show the possibility of quantum interference between the probability amplitudes for a pair of photons with different frequencies in the coherent Raman process. We assume that the sidebands 0 and 1 are initially prepared in independent single-photon states. This initial condition corresponds to the situation where two photons with different frequencies  $\omega_0$  and  $\omega_1$  are incident into the Raman medium. The input state of the fields can be written as

$$|\Psi_{in}\rangle = |1\rangle_0 |1\rangle_1 \prod_{q \neq 0,1} |0\rangle_q = \hat{b}_0^\dagger(0) \hat{b}_1^\dagger(0) |0\rangle. \quad (30)$$

The output state of the fields is given by  $|\Psi_{out}\rangle = \hat{b}_0^\dagger(-L/c) \hat{b}_1^\dagger(-L/c) |0\rangle$ . With the help of Eq. (6), we find

$$\begin{aligned} |\Psi_{out}\rangle = & -i\sqrt{2} \sum_q e^{iq\pi} J_q(\kappa L) J_{q-1}(\kappa L) |2_q\rangle \\ & -i \sum_{k < l} e^{i(k+l)\pi/2} [J_k(\kappa L) J_{l-1}(\kappa L) \\ & + J_l(\kappa L) J_{k-1}(\kappa L)] |1_k 1_l\rangle. \end{aligned} \quad (31)$$

Here, the Fock state  $|2_q\rangle$  is the state of two photons in the sideband  $q$  with no photons in the other sidebands, and the Fock state  $|1_k 1_l\rangle$  is the state in which there is one photon in each of the sidebands  $k$  and  $l$  but no photons in the other sidebands.

The probability for finding two photons in the sideband  $q$  is given by  $W_q^{(2)} = 2J_q^2(\kappa L) J_{q-1}^2(\kappa L)$ . The joint probability for finding one photon in each of the sidebands  $k$  and  $l$  ( $k \neq l$ ) is

$$W_{kl} = [J_k(\kappa L) J_{l-1}(\kappa L) + J_l(\kappa L) J_{k-1}(\kappa L)]^2. \quad (32)$$

The probability  $W_q^{(1)} = \sum_{l \neq q} W_{ql}$  for having one and only one photon in the sideband  $q$  is  $W_q^{(1)} = J_q^2(\kappa L) + J_{q-1}^2(\kappa L) - 4J_q^2(\kappa L) J_{q-1}^2(\kappa L)$ . The mean photon number of the sideband  $q$  is  $\langle \hat{n}_q \rangle = J_q^2(\kappa L) + J_{q-1}^2(\kappa L)$ . We find the relations  $W_{-q}^{(2)} = W_{1+q}^{(2)}$ ,  $W_{-q}^{(1)} = W_{1+q}^{(1)}$ , and  $\langle \hat{n}_{-q} \rangle = \langle \hat{n}_{1+q} \rangle$ , which reflect the symmetry of the generated Stokes and anti-Stokes sidebands with respect to the two input sidebands 0 and 1.

When we insert  $k=0$  and  $l=1$  into Eq. (32), we obtain the following expression for the joint probability for finding one photon in each of the sidebands 0 and 1:

$$W_{01} = [J_0^2(\kappa L) - J_1^2(\kappa L)]^2. \quad (33)$$

This expression shows that the joint probability  $W_{01}$  may become zero at certain values of  $\kappa L$  (see Fig. 7). This is a

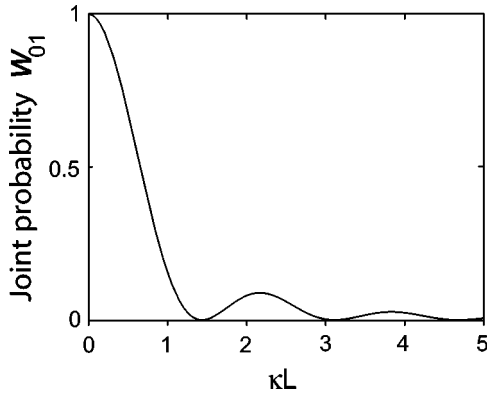


FIG. 7. Joint probability  $W_{01}$  for finding one photon in each of the sidebands 0 and 1 as a function of the effective medium length  $\kappa L$ .

signature of destructive interference between two channels that form the state  $|1_0 1_1\rangle$ . In the first channel, each of the two photons individually transmits through the medium without any changes. The two-photon probability amplitude for this channel is  $J_0(\kappa L)J_0(\kappa L) = J_0^2(\kappa L)$ . In the second channel, both the photons are scattered from the prepared Raman coherence and exchange their sidebands. The two-photon probability amplitude for this channel is  $e^{i\pi/2}J_1(\kappa L)e^{i\pi/2}J_1(\kappa L) = -J_1^2(\kappa L)$ . Since Raman scattering produces a phase shift of  $\pi/2$  for each photon, the probability amplitudes for the two channels (the transmission and scattering of both the photons) are  $180^\circ$  out of phase. The interference between the two channels is therefore destructive, yielding the output state  $|1_0 1_1\rangle$  with the joint probability  $W_{01}$  given above. When the medium length  $L$  is such that  $J_0^2(\kappa L) = J_1^2(\kappa L)$ , the interference between the two two-photon amplitudes becomes completely destructive, and therefore the state  $|1_0 1_1\rangle$  is removed from the output state (31). We denote such a medium length by  $L_f$ . The positions of the zeros of  $W_{01}$  depicted in Fig. 7 indicate that the first three values of  $L_f$  are given by  $\kappa L_f = 1.44, 3.11, \text{ and } 4.68$ . It is interesting to note that  $\kappa L_f$  can be determined by an experiment using a single-mode input. Indeed, in the case where a single sideband 0 is initially excited, the mean photon numbers of the generated sidebands are given by Eq. (9). Therefore the effective medium length  $\kappa L_f$  corresponds to the situation where the probe sideband 0 and its adjacent sidebands  $\pm 1$  have the same mean photon numbers at the output.

There exist literatures on two-photon interference in various systems [15,16,23]. Two-photon interference in coherent Raman scattering, described above, is an analogy of two-photon interference at a conventional beam splitter [15,19]. We emphasize that two-photon interference in coherent Raman scattering involves copropagating photons with different frequencies in a collinear scheme.

#### D. General relation between the $P$ representations of the input and output states

To be more general, we consider the case where an arbitrary number of sidebands is initially excited. We find that an

arbitrary multimode coherent state  $|\{\alpha_q(0)\}\rangle$  of the input fields produces a coherent state  $|\{\alpha_q(L/c)\}\rangle$  of the output fields. Here, the output amplitudes  $\{\alpha_q(L/c)\}$  are linearly transformed from the input amplitudes  $\{\alpha_q(0)\}$  as given by

$$\alpha_q(L/c) = \sum_{q'} e^{i(q-q')\pi/2} J_{q-q'}(\kappa L) \alpha_{q'}(0). \quad (34)$$

Consequently, the diagonal coherent-state representation  $P_{\text{in}}(\{\alpha_q\})$  of an arbitrary input quantum state  $\hat{\rho}_{\text{in}}$  determines the representation  $P_{\text{out}}(\{\alpha_q\})$  of the output state  $\hat{\rho}_{\text{out}}$  via the equation

$$P_{\text{out}}(\{\alpha_q\}) = P_{\text{in}}(\{\alpha'_q\}). \quad (35)$$

Here, we have introduced the notation

$$\alpha'_q = \sum_{q'} e^{-i(q-q')\pi/2} J_{q-q'}(\kappa L) \alpha_{q'}. \quad (36)$$

If the input state  $\hat{\rho}_{\text{in}}$  is a classical state [19],  $P_{\text{in}}(\{\alpha_q\})$  must be non-negative and less singular than a  $\delta$  function, and consequently so must  $P_{\text{out}}(\{\alpha_q\})$ . In this case, the output state  $\hat{\rho}_{\text{out}}$  is also a classical state. Moreover, since the multimode coherent state  $|\{\alpha_q\}\rangle$  is separable and the weight factor  $P_{\text{out}}(\{\alpha_q\})$  is non-negative, the output state  $\hat{\rho}_{\text{out}}$  is, by definition, separable [24,25]. Therefore a necessary condition for the output fields to be in an inseparable (entangled) state or, more generally, in a nonclassical state is that the input field state is a nonclassical state. A similar condition has been derived for the beam splitter entangler [17]. Note that, in the case where we use a single-mode input field with  $q=0$ , prepared in an arbitrary quantum state with the coherent-state representation  $P_{\text{in}}^{(0)}(\alpha)$  (the Stokes and anti-Stokes sideband fields are initially in the vacuum state), Eq. (35) becomes  $P_{\text{out}}(\{\alpha_q\}) = P_{\text{in}}^{(0)}(\alpha'_0) \prod_{q \neq 0} \delta(\alpha'_q)$ .

#### V. PRODUCTION OF A MULTIPARTITE ENTANGLED COHERENT STATE

In this section, we show that the coherent Raman scattering can produce a multipartite entangled coherent state if the probe field is initially prepared in an odd or even coherent state. Entangled coherent states [26–34] of the electromagnetic field have attracted considerable interest for quantum communication purposes. Entanglement properties of two-mode entangled coherent states have been studied [27,28]. In the context of these states, teleportation [28], entanglement purification [29], Bell-inequality violations [30], and universal quantum computing [31] have been discussed. The multipartite generalizations [32] of entangled coherent states and their photon statistical properties [33] have been examined. It has been shown that entangled coherent states can be generated in schemes using a nonlinear interferometer [26,32] or a double electromagnetically induced transparency system [34].

We assume that the probe field is initially in an even or odd superposition of coherent states [35]

$$|\Psi_{\text{in}}\rangle_0 = N_\nu(|\alpha\rangle_0 + \nu|-\alpha\rangle_0), \quad (37)$$

i.e., a Schrödinger cat state, while the other sideband fields are initially in the vacuum state. Here, we have introduced the notation  $\nu = \pm 1$ , where the plus and minus signs correspond to the even and odd coherent states, respectively. The normalization constant  $N_\nu$  is given as  $N_\nu = (2 + 2\nu e^{-2|\alpha|^2})^{-1/2}$ . Note that Schrödinger cat states have been produced in the microwave cavity field [36], the center-of-mass vibrational motion of a trapped ion [37], and the radial excitation of an electron in a Rydberg state [38]. A great variety of methods have been proposed for generating Schrödinger cat states in the optical domain [39].

For the input state (37), we obtain the output state

$$|\Psi_{\text{out}}\rangle = N_\nu[|\{\alpha_q\}\rangle + \nu|-\alpha_q\rangle]. \quad (38)$$

Here,  $|\{\alpha_q\}\rangle$  and  $|-\alpha_q\rangle$  are multimode coherent states, with the amplitudes

$$\alpha_q = \alpha J_q(\kappa L) e^{iq\pi/2}. \quad (39)$$

Equation (38) stands for a multimode even or odd coherent state [33], which is also a multipartite entangled coherent state [32]. Note that the multipartite entangled coherent state studied in [32] involves a finite number of modes with equal mode amplitudes. Meanwhile, the output state (38) involves an infinite number of modes with a Bessel-function distribution of mode amplitudes. Such a mode amplitude distribution results from the coherent-Raman-scattering process. Unlike the techniques based on a nonlinear interferometer [32] or a double electromagnetically induced transparency system [34], the Raman technique does not require multiparticle Bell-state measurements, and therefore is simple and efficient. In addition, the Raman technique allows us to generate multipartite entanglement between the sideband fields with different frequencies, unlike the nonlinear interferometer method [32].

We examine the bipartite entanglement of the generated multimode state (38). We follow the procedures of Wang and Sanders [32] to calculate the so-called concurrence [40], which is a measure of bipartite entanglement. We consider the bipartite reduced density matrix  $\hat{\rho}_{kl}$  obtained from the density matrix  $|\Psi_{\text{out}}\rangle\langle\Psi_{\text{out}}|$  by tracing out all sidebands except for the two sidebands  $k$  and  $l$  (with  $k \neq l$ ). Using Eq. (38), we find

$$\begin{aligned} \hat{\rho}_{kl} = & N_\nu^2 [|\alpha_k, \alpha_l\rangle\langle\alpha_k, \alpha_l| + |-\alpha_k, -\alpha_l\rangle\langle-\alpha_k, -\alpha_l| \\ & + \nu Q (|\alpha_k, \alpha_l\rangle\langle-\alpha_k, -\alpha_l| + |-\alpha_k, -\alpha_l\rangle\langle\alpha_k, \alpha_l|)], \end{aligned} \quad (40)$$

where  $Q = \exp(-2|\alpha|^2 + 2|\alpha_k|^2 + 2|\alpha_l|^2)$ . For the bipartite mixed state described by the density matrix  $\hat{\rho}_{kl}$ , the concurrence is defined as [40]

$$C_{kl} = \max\{\lambda_1 - \lambda_2 - \lambda_3 - \lambda_4, 0\}, \quad (41)$$

where  $\lambda_1, \lambda_2, \lambda_3$ , and  $\lambda_4$  are the square roots of the eigenvalues, in decreasing order, of the matrix

$$\hat{R}_{kl} = \hat{\rho}_{kl}(\hat{\sigma}_y \otimes \hat{\sigma}_y) \hat{\rho}_{kl}^* (\hat{\sigma}_y \otimes \hat{\sigma}_y). \quad (42)$$

Here,  $\hat{\sigma}_y = \begin{pmatrix} 0 & -i \\ i & 0 \end{pmatrix}$  is a Pauli matrix in the standard basis of a qubit, and  $\hat{\sigma}_y \otimes \hat{\sigma}_y$  is the spin-flip operator for two qubits.

We choose an orthogonal qubit basis  $\{|\mathbf{0}_q\rangle, |\mathbf{1}_q\rangle\}$  for each sideband  $q$ . We distinguish this basis from the Fock states, employed earlier, by using boldface symbols. For the sideband  $k$ , the qubit basis is defined as  $|\mathbf{0}_k\rangle \equiv |\alpha_k\rangle$  and  $|\mathbf{1}_k\rangle \equiv (|-\alpha_k\rangle - p_k|\alpha_k\rangle)/M_k$ . For the sideband  $l$ , the qubit basis is defined as  $|\mathbf{0}_l\rangle \equiv |-\alpha_l\rangle$  and  $|\mathbf{1}_l\rangle \equiv (|\alpha_l\rangle - p_l|-\alpha_l\rangle)/M_l$ . Here, we have introduced the notation  $p_q = e^{-2|\alpha_q|^2}$  and  $M_q = \sqrt{1 - p_q^2}$ . It then follows that, for the sideband  $k$ , one has  $|\alpha_k\rangle = |\mathbf{0}_k\rangle$  and  $|-\alpha_k\rangle = M_k|\mathbf{1}_k\rangle + p_k|\mathbf{0}_k\rangle$ , while, for the sideband  $l$ , one has  $|-\alpha_l\rangle = |\mathbf{0}_l\rangle$  and  $|\alpha_l\rangle = M_l|\mathbf{1}_l\rangle + p_l|\mathbf{0}_l\rangle$ . Then, in the standard basis  $\{|\mathbf{0}_k\mathbf{0}_l\rangle, |\mathbf{0}_k\mathbf{1}_l\rangle, |\mathbf{1}_k\mathbf{0}_l\rangle, |\mathbf{1}_k\mathbf{1}_l\rangle\}$  of the two qubits, Eq. (42) yields

$$\hat{R}_{kl} = N_\nu^4 M_k M_l \begin{pmatrix} 0 & A_{kl} & A_{lk} & -B \\ 0 & D & F_l & -A_{lk} \\ 0 & F_k & D & -A_{kl} \\ 0 & 0 & 0 & 0 \end{pmatrix}, \quad (43)$$

where  $A_{kl} = M_k[p_l(1 + Q^2) + 2\nu Q p_k]$ ,  $B = 2(p_k + \nu Q p_l)(p_l + \nu Q p_k)$ ,  $D = M_k M_l(1 + Q^2)$ , and  $F_k = 2\nu Q M_k^2$ . The square roots of the eigenvalues of  $\hat{R}_{kl}$  are  $\lambda_1 = N_\nu^2 M_k M_l(1 + Q)$ ,  $\lambda_2 = N_\nu^2 M_k M_l(1 - Q)$ , and  $\lambda_3 = \lambda_4 = 0$ . Then, we find from Eq. (41) that the concurrence is  $C_{kl} = 2N_\nu^2 M_k M_l Q$ . When we use the explicit expressions for  $N_\nu$ ,  $M_q$ , and  $Q$ , we obtain

$$\begin{aligned} C_{kl} = & [\exp(2|\alpha|^2) + \nu]^{-1} \{\exp[4|\alpha|^2 J_k^2(\kappa L)] - 1\}^{1/2} \\ & \times \{\exp[4|\alpha|^2 J_l^2(\kappa L)] - 1\}^{1/2}. \end{aligned} \quad (44)$$

Unlike the case of a finite number of modes with equal mode amplitudes [32], the expression (44) for the concurrence contains the Bessel functions, which result from the scattering amplitudes of the modes. It is clear from the expression (44) that an odd coherent state ( $\nu = -1$ ) of the input can produce a larger bipartite entanglement than an even coherent state ( $\nu = 1$ ) can. In addition, when we increase the medium length  $L$  or the sideband order  $k$  or  $l$ , the concurrence  $C_{kl}$  undergoes oscillations as described by the Bessel functions  $J_k(\kappa L)$  and  $J_l(\kappa L)$ , and tends to zero in the limit  $L \rightarrow \infty$ . One can show that  $0 \leq C_{kl} \leq 1$  (for  $k \neq l$ ), that is, the state (38) does not possess more than one ebit of bipartite entanglement. For the higher sideband orders, the onset of generation of the sidebands occurs later and hence so does the onset of the entanglement between them.

For two conjugate anti-Stokes and Stokes sidebands (the pair of sidebands  $k$  and  $-k$ , where  $k \neq 0$ ), Eq. (44) yields

$$C_{k,-k} = \frac{\exp[4|\alpha|^2 J_k^2(\kappa L)] - 1}{\exp(2|\alpha|^2) + \nu}. \quad (45)$$

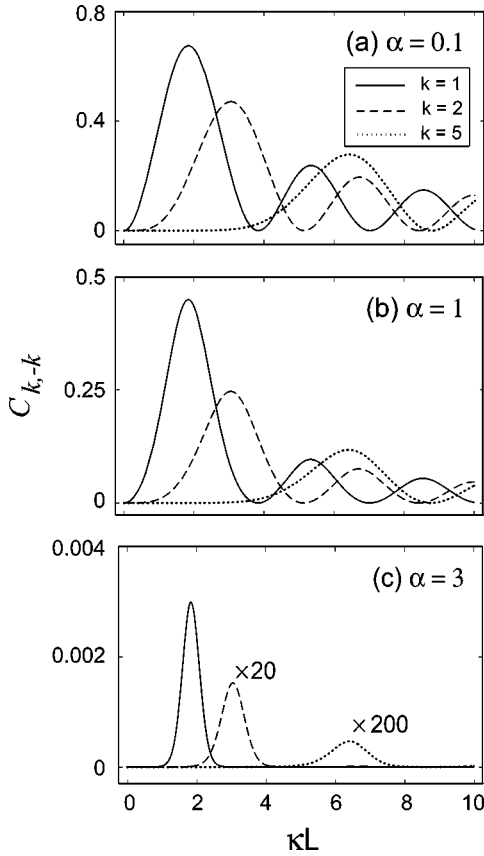


FIG. 8. Concurrence  $C_{k,-k}$  for different conjugate-sideband pairs  $(k, -k)$  and for various values of the input probe field amplitude  $\alpha$ . The probe field is initially in an odd coherent state ( $\nu = -1$ ). In (c) we have amplified  $C_{2,-2}$  and  $C_{5,-5}$  by 20 and 200 times, respectively.

Since  $J_0^2(x) + 2\sum_{k=1}^{\infty} J_k^2(x) = 1$ , the set of the concurrences  $C_{k,-k}$  for all possible conjugate-sideband pairs satisfies the following relation:

$$\prod_{k=1}^{\infty} [1 + (e^{2|\alpha|^2} + \nu)C_{k,-k}] = \exp\{2|\alpha|^2[1 - J_0^2(\kappa L)]\}. \quad (46)$$

We denote by  $x_k$  the value of  $x$  at which the Bessel function  $J_k(x)$  reaches its largest absolute value. Then, the concurrence  $C_{k,-k}$  (with  $k \neq 0$ ) reaches its largest value at the optimal medium length  $L_k = x_k/\kappa$ . The higher the sideband order  $k$ , the larger is the optimal length  $L_k$  and the smaller is the maximal value of  $C_{k,-k}$ .

In Fig. 8, we plot the conjugate-sideband concurrence  $C_{k,-k}$  as a function of the effective medium length  $\kappa L$ . Clearly, the maximum entanglement of the sideband pair  $(k, -k)$  is attained at the first peak of the Bessel function  $J_k(x)$ . As seen from the figure and as can be shown analytically, in the case of odd coherent states, the amount of entanglement between the sidebands decreases with the increase of the probe field amplitude. In Figs. 8(a) and (b), we observe oscillations in  $C_{k,-k}$  that are due to the dependence of this quantity on the Bessel function  $J_k$ . However, such

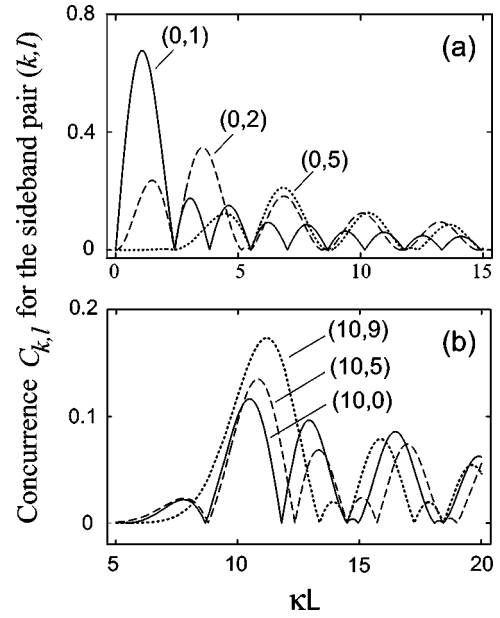


FIG. 9. Concurrence  $C_{k,l}$  for various asymmetric-order sideband pairs  $(k, l)$  ( $k \neq \pm l$ ). The pairs are (a) the probe and one of the other sidebands and (b) the tenth anti-Stokes sideband and one of the other sidebands. The probe field is initially in an odd coherent state ( $\nu = -1$ ), with the amplitude  $\alpha = 0.1$ .

oscillations are insignificant in Fig. 8(c), where the probe field amplitude is rather large.

In Fig. 9, we plot the concurrence  $C_{k,l}$  for various asymmetric-order sideband pairs ( $k \neq \pm l$ ). The most distinct feature of this case as compared to the case of symmetric (conjugate) pairs [Eq. (45) and Fig. 8] is that the condition for maximum entanglement is governed by the interference between the Bessel functions of different orders, and hence the first peak in  $C_{k,l}$  need not be the absolute maximum for a given pair  $(k, l)$ . Furthermore, Fig. 9(b) shows that, for a sideband pair  $(k, l)$  with a given  $k \neq 0$ , the largest achievable entanglement need not be obtained for  $l = 0$  (the input probe field).

We evaluate the concurrence  $C_{kl}$  for an arbitrary sideband pair  $(k, l)$  in the limit of large  $|\alpha|$ . Under the conditions  $|\alpha|, |\alpha J_k(\kappa L)|, |\alpha J_l(\kappa L)| \gg 1$ , we find from Eq. (44) the estimate  $C_{kl} = \exp\{-2|\alpha|^2[1 - J_k^2(\kappa L) - J_l^2(\kappa L)]\}$ . This expression says that  $C_{kl}$  tends to zero in the limit of large  $|\alpha|$ .

In the limit  $|\alpha| \ll 1$ , we expand the expression (44) into a series of  $|\alpha|$  and keep only the first nonvanishing term. In the case of  $\nu = 1$  (even coherent state), we find the estimate  $C_{kl} = 2|\alpha|^2 |J_k(\kappa L)J_l(\kappa L)|$ , which tends to zero in the limit  $|\alpha| \rightarrow 0$ . This asymptotic behavior is due to the fact that, in the limit  $|\alpha| \rightarrow 0$ , the even coherent state approaches the vacuum state  $|0\rangle$ . Meanwhile, in the case of  $\nu = -1$  (odd coherent state), the value of  $C_{kl}$  in the limit  $|\alpha| \rightarrow 0$  is  $C_{kl} = 2|J_k(\kappa L)J_l(\kappa L)|$ . This bipartite concurrence is nonzero except for the medium lengths at which either  $J_k(\kappa L)$  or  $J_l(\kappa L)$  is zero. This nonzero asymptotic value is due to the fact that, in the limit  $|\alpha| \rightarrow 0$ , the odd coherent state of the input field approaches the single-photon state  $|1\rangle$ , and consequently the output field state approaches the state  $|W_R\rangle$

$\equiv \sum_q J_q(\kappa L) e^{iq\pi/2} |1_q\rangle$ . Thus the multipartite entangled state  $|W_R\rangle$  can be generated by high-order coherent Raman scattering of a single photon. This state is similar to the so-called  $W$  state [32,41]. Unlike the state  $W$ , which is a symmetric single-excitation superposition state of a finite number of qubits, the state  $|W_R\rangle$  involves an infinite number of sidebands, weighted by the Bessel functions.

## VI. CONCLUSIONS AND DISCUSSIONS

We have studied the quantum properties of multiorder sidebands generated by the beating of a quantum probe field with a prepared Raman coherence in a far-off-resonance medium. Under the conditions of negligible dispersion and limited bandwidth, we have derived a Bessel-function solution for the sideband field operators. We have examined the quantum properties of the sideband fields in the case of single-mode quantum input. We have shown that, when we change the effective medium length or the Raman sideband order, the autocorrelation functions, the cross-correlation functions, the photon distributions, and the squeezing factors undergo oscillations governed by the Bessel functions. However, the normalized autocorrelation functions and normalized squeezing factors of the probe field are not altered by the parametric beating process, and are replicated into the comb of generated sidebands. Therefore the multiorder coherent Raman process can be used to multiplex the statistical properties of a quantum probe field into a broad comb of different frequencies.

We have studied the mixing and modulation of photon statistical properties in the case of two-mode quantum input. We have shown that the prepared Raman coherence and the medium length can be used as control parameters to switch a sideband field from one type of photon statistics to another

type, or from a nonsqueezed state to a squeezed state and vice versa. In addition, we can switch nonclassical properties from one frequency to another frequency. We have shown an example of quantum interference between the probability amplitudes for two photons with different frequencies.

We have investigated the bipartite entanglement of multiorder sidebands generated by the coherent Raman scattering of a quantum probe field prepared in an even or odd coherent state. We have shown that the concurrence for a pair of conjugate sidebands reaches a maximum value at an optimal medium length that is determined by the medium coherence and the Raman sideband order.

The ability of the far-off-resonance Raman medium to generate a broad comb of fields with similar quantum statistical properties and to switch the quantum statistical characteristics of the radiation fields from one type to another type may find useful applications for high-performance optical communication networks. In addition, two-photon interference in coherent Raman scattering may find various applications for high-precision measurements and also for quantum computation. We emphasize that the coupling between the Raman sidebands can be controlled by the magnitude of the prepared Raman coherence, that is, by the intensities of the driving fields. In a realistic far-off-resonance Raman medium, such as molecular hydrogen or deuterium vapor [5,6], solid hydrogen [7,8], and rare-earth doped dielectrics [10], a large Raman coherence and, consequently, a large number of Raman sidebands can be generated by the two-color adiabatic pumping technique. In such a system, the generation of a broad comb of high-order Raman sidebands with nonclassical properties is, in principle, feasible. Therefore we expect that the coherent-Raman-scattering technique using quantum fields will become a practical and efficient method for a wide range of applications in nonlinear and quantum optics.

- 
- [1] V.P. Kalosha and J. Herrmann, Phys. Rev. Lett. **85**, 1226 (2000); Opt. Lett. **26**, 456 (2001); Fam Le Kien, Nguyen Hong Shon, and K. Hakuta, Phys. Rev. A **64**, 051803(R) (2001); Fam Le Kien, K. Hakuta, and A.V. Sokolov, *ibid.* **66**, 023813 (2002); V. Kalosha, M. Spanner, J. Herrmann, and M. Ivanov, Phys. Rev. Lett. **88**, 103901 (2002); R.A. Bartels, T.C. Weinacht, N. Wagner, M. Baertschy, Chris H. Greene, M.M. Murnane, and H.C. Kapteyn, *ibid.* **88**, 013903 (2002).
  - [2] J.Q. Liang, M. Katsuragawa, Fam Le Kien, and K. Hakuta, Phys. Rev. Lett. **85**, 2474 (2000).
  - [3] M. Katsuragawa, J.Q. Liang, Fam Le Kien, and K. Hakuta, Phys. Rev. A **65**, 025801 (2002).
  - [4] A. Nazarkin, G. Korn, M. Wittmann, and T. Elsaesser, Phys. Rev. Lett. **83**, 2560 (1999).
  - [5] S.E. Harris and A.V. Sokolov, Phys. Rev. A **55**, R4019 (1997); A.V. Sokolov, D.D. Yavuz, and S.E. Harris, Opt. Lett. **24**, 557 (1999); A.V. Sokolov, D.D. Yavuz, D.R. Walker, G.Y. Yin, and S.E. Harris, Phys. Rev. A **63**, 051801(R) (2001).
  - [6] A.V. Sokolov, D.R. Walker, D.D. Yavuz, G.Y. Yin, and S.E. Harris, Phys. Rev. Lett. **85**, 562 (2000).
  - [7] S.E. Harris and A.V. Sokolov, Phys. Rev. Lett. **81**, 2894 (1998).
  - [8] Fam Le Kien, J.Q. Liang, M. Katsuragawa, K. Ohtsuki, K. Hakuta, and A.V. Sokolov, Phys. Rev. A **60**, 1562 (1999).
  - [9] Fam Le Kien and K. Hakuta, Phys. Rev. A **67**, 033808 (2003).
  - [10] R. Kolesov and O. Kocharovskaya, Phys. Rev. A **67**, 023810 (2003).
  - [11] A.V. Sokolov, D.R. Walker, D.D. Yavuz, G.Y. Yin, and S.E. Harris, Phys. Rev. Lett. **87**, 033402 (2001).
  - [12] N. Zhavoronkov and G. Korn, Phys. Rev. Lett. **88**, 203901 (2002).
  - [13] S.E. Harris, D.R. Walker, and D.D. Yavuz, Phys. Rev. A **65**, 021801(R) (2002).
  - [14] H.P. Yuen and J.H. Shapiro, IEEE Trans. Inf. Theory **IT-26**, 78 (1980); M. Ley and R. Loudon, Opt. Commun. **54**, 317 (1985); B. Yurke, S.L. McCall, and J.R. Klauder, Phys. Rev. A **33**, 4033 (1986); S. Prasad, M.O. Scully, and W. Martienssen, Opt. Commun. **62**, 139 (1987); Z.Y. Ou, C.K. Hong, and L. Mandel, *ibid.* **63**, 118 (1987); H. Fearn and R. Loudon, *ibid.* **64**, 485 (1987); R.A. Campos, B.E.A. Saleh, and M.C. Teich, Phys. Rev. A **40**, 1371 (1989).
  - [15] C.K. Hong, Z.Y. Ou, and L. Mandel, Phys. Rev. Lett. **59**, 2044 (1987).

- [16] J. Torgerson, D. Branning, C. Monken, and L. Mandel, *Phys. Lett. A* **204**, 323 (1995); K. Mattle, H. Weinfurter, P.G. Kwiat, and A. Zeilinger, *Phys. Rev. Lett.* **76**, 4656 (1996); D. Bouwmeester, J. Pan, K. Mattle, M. Eibl, H. Weinfurter, and A. Zeilinger, *Nature (London)* **390**, 575 (1997); T.C. Ralph, N.K. Langford, T.B. Bell, and A.G. White, *Phys. Rev. A* **65**, 062324 (2002); T.B. Pittman, B.C. Jacobs, and J.D. Franson, *Phys. Rev. Lett.* **88**, 257902 (2002); S.P. Walborn, A.N. de Oliveira, S. Padua, and C.H. Monken, *ibid.* **90**, 143601 (2003).
- [17] M.S. Kim, W. Son, V. Bužek, and P.L. Knight, *Phys. Rev. A* **65**, 032323 (2002); Wang Xiang-bin, *ibid.* **66**, 024303 (2002).
- [18] W.K. Lai, V. Bužek, and P.L. Knight, *Phys. Rev. A* **43**, 6323 (1991); Janszky, C. Sibia, and M. Bertolotti, *J. Mod. Opt.* **35**, 1757 (1988).
- [19] L. Mandel and E. Wolf, *Optical Coherence and Quantum Optics* (Cambridge University Press, New York, 1995); M. Scully and S. Zubairy, *Quantum Optics* (Cambridge University Press, New York, 1997).
- [20] L.J. Wang, C.K. Hong, and S.R. Friberg, *J. Opt. B: Quantum Semiclassical Opt.* **3**, 346 (2001).
- [21] M.D. Lukin, A.B. Matsko, M. Fleischhauer, and M.O. Scully, *Phys. Rev. Lett.* **82**, 1847 (1999); A.S. Zibrov, A.B. Matsko, O. Kocharovskaya, Y.V. Rostovtsev, G.R. Welch, and M.O. Scully, *ibid.* **88**, 103601 (2002).
- [22] A.H. Toor and M.S. Zubairy, *Phys. Rev. A* **45**, 4951 (1992).
- [23] Z.Y. Ou and L. Mandel, *Phys. Rev. Lett.* **61**, 54 (1988); **62**, 2941 (1989); H. Huang and J.H. Eberly, *J. Mod. Opt.* **40**, 915 (1993); M.O. Scully, U.W. Rathe, C. Su, and G.S. Agarwal, *Opt. Commun.* **136**, 39 (1997); A.K. Patnaik and G.S. Agarwal, *J. Mod. Opt.* **45**, 2131 (1998).
- [24] *The Physics of Quantum Information*, edited by D. Bouwmeester, A. K. Ekert, and A. Zeilinger (Springer, New York, 2000).
- [25] M. A. Nielsen and I. L. Chuang, *Quantum Computation and Quantum Information* (Cambridge University Press, New York, 2000).
- [26] B.C. Sanders, *Phys. Rev. A* **45**, 6811 (1992); B.C. Sanders and D.A. Rice, *ibid.* **61**, 013805 (2000); W.J. Munro, G.J. Milburn, and B.C. Sanders, *ibid.* **62**, 052108 (2000); J.C. Howell and J.A. Yeazell, *ibid.* **62**, 012102 (2000).
- [27] B.C. Sanders, K.S. Lee, and M.S. Kim, *Phys. Rev. A* **52**, 735 (1995); O. Hirota and M. Sasaki, Report No. quant-ph/0101018; O. Hirota, S.J. van Enk, K. Nakamura, M. Sohma, and K. Kato, Report No. quant-ph/0101096.
- [28] X. Wang, *Phys. Rev. A* **64**, 022302 (2001); S.J. van Enk and O. Hirota, *ibid.* **64**, 022313 (2001).
- [29] J. Clausen, L. Knöll, and D.-G. Welsch, *Phys. Rev. A* **66**, 062303 (2002).
- [30] A. Mann, B.C. Sanders, and W.J. Munro, *Phys. Rev. A* **51**, 989 (1995); D. Wilson, H. Jeong, and M.S. Kim, *J. Mod. Opt.* **49**, 851 (2002).
- [31] H. Jeong and M.S. Kim, *Phys. Rev. A* **65**, 042305 (2002).
- [32] X. Wang and B.C. Sanders, *Phys. Rev. A* **65**, 012303 (2002).
- [33] N.A. Ansari and V.I. Manko, *Phys. Rev. A* **50**, 1942 (1994); V.V. Dodonov, V.I. Manko, and D.E. Nikonov, *ibid.* **51**, 3328 (1995).
- [34] M. Paternostro, M.S. Kim, and B.S. Ham, *Phys. Rev. A* **67**, 023811 (2003).
- [35] V. Bužek, A. Vidiella-Barranco, and P.L. Knight, *Phys. Rev. A* **45**, 6570 (1992).
- [36] M. Brune, E. Hagley, J. Dreyer, X. Maitre, A. Maali, C. Wunderlich, J.M. Raimond, and S. Haroche, *Phys. Rev. Lett.* **77**, 4887 (1996).
- [37] C. Monroe, D.M. Meekhof, B.E. King, and D.J. Wineland, *Science* **272**, 1131 (1996).
- [38] M.W. Noel and C.R. Stroud, Jr., *Phys. Rev. Lett.* **77**, 1913 (1996).
- [39] See, for example, M. Dakna, T. Anhut, T. Opatrny, L. Knöll, and D.-G. Welsch, *Phys. Rev. A* **55**, 3184 (1997); P.T. Cochrane, G.J. Milburn, and W.J. Munro, *ibid.* **59**, 2631 (1999); C.C. Gerry, *ibid.* **59**, 4095 (1999).
- [40] S. Hill and W.K. Wootters, *Phys. Rev. Lett.* **78**, 5022 (1997); W.K. Wootters, *ibid.* **80**, 2245 (1998).
- [41] C.H. Bennett, H.J. Bernstein, S. Popescu, and B. Schumacher, *Phys. Rev. A* **53**, 2046 (1996).